

Supplementary Information

**The Role of Sodium in Stabilizing Tin-Lead (Sn-Pb) Alloyed
Perovskite Quantum Dots**

Junke Jiang,^{1,2,a} Feng Liu,^{3,a} Qing Shen,^{*,4} and Shuxia Tao,^{*,1,2}

¹Materials Simulation and Modelling, Department of Applied Physics, Eindhoven University of Technology, 5600MB Eindhoven, The Netherlands

²Center for Computational Energy Research, Department of Applied Physics, Eindhoven University of Technology, Eindhoven 5600 MB, The Netherlands

³Institute of Molecular Sciences and Engineering, Shandong University, Qingdao 266237, P.R. China

⁴Faculty of Informatics and Engineering, The University of Electro-Communications, 1-5-1 Chofugaoka, Tokyo 182-8585, Japan

^aThese authors contributed equally to this work

*Correspondence authors: S.X.Tao@tue.nl (Shuxia Tao); shen@pc.uec.ac.jp (Qing Shen)

Computational details

Vacancy formation energy. For Na doping, we replace one Cs⁺ cation with Na⁺. We calculate the formation energies of I and Sn vacancies at the CsI-terminated surface and MI₂-terminated surface (M: Sn or Pb) of this structure. As references, we also calculate the same formation energy of unmodified CsI- and MI₂-terminated surfaces. The details of the procedure are as follows. The defect formation energy of an ion (I anion, Sn cation, or Pb cation) is defined as:

$$\Delta E_{\text{vac}} [\text{ion}] = E_{\text{tot}} [\text{ion-vac}] - (E_{\text{tot}} [\text{surface}] - \mu[\text{ion}]) + qE_{\text{Fermi}} \quad (1)$$

where $E_{\text{tot}} [\text{ion-vac}]$ and $E_{\text{tot}} [\text{surface}]$ are the total energies of the surfaces with and without ion vacancy, respectively, and E_{Fermi} and $\mu[\text{ion}]$ are the Fermi energy and the chemical potential of the ion, respectively. The E_{Fermi} and $\mu[\text{ion}]$ is assumed to be the same for all perovskites. This approximation is valid because, in our experiments,¹ the important parameters (e.g., precursor concentration, the source of ions, and synthesis temperature) during the synthesis process of these perovskites are kept the same.

We define the suppression of ion vacancy formation^{2,3} due to the introduction of Na⁺, as:

$$\Delta\Delta E_{\text{vac}} = \Delta E_{\text{vac}} [\text{ion}] [\text{Na}] - \Delta E_{\text{vac}} [\text{ion}][\text{ref}] \quad (2)$$

where $\Delta E_{\text{vac}} [\text{ion}] [\text{Na}]$ is the formation energy of an ion defect in the presence of Na, and $\Delta E_{\text{vac}} [\text{ion}][\text{ref}]$ represents one of the unmodified CsI-terminated surfaces or unmodified MI₂-terminated surfaces.

Ligand binding energy. The binding energy (E_b) of the ligands to the QDs surface is computed as

$$E_b = (E_{\text{tot}} - E_{\text{per}} - E_{\text{lig}})/S \quad (3)$$

where E_{tot} is the energy of the slab model passivated with ligands, E_{per} the energy of the slab model without the ligand, and E_{lig} the energy of the ligand, and S is the surface area of the interfaces. The more negative the E_b , the stronger the binding strength between the ligand and the QDs.

Charge displacement curve. The binding of perovskites and ligands will cause the charge redistribution at the interface. To analyze the charge redistribution, the charge density difference $\Delta\rho$ is calculated by:

$$\Delta\rho = \Delta\rho_{\text{tot}} - \Delta\rho_{\text{per}} - \Delta\rho_{\text{lig}} \quad (4)$$

where ρ_{tot} , ρ_{per} , and ρ_{lig} denote the charge density of the optimized perovskite/ligand structure, the separated perovskite slab, and the separated ligand layer, respectively. To investigate the charge redistribution between the ligand and the perovskite, the plane-averaged charge density difference $\Delta\rho_{\text{avg}}(z)$ is defined as:

$$\Delta\rho_{avg}(z) = \sum_{ij} dx dy \Delta\rho = \sum_{ij} \Delta x_i \Delta y_i \Delta\rho_{i,j}$$
(5)

the positive and negative signals of $\Delta\rho_{avg}(z)$ represent electron accumulation and depletion along the z-direction, respectively. Then, the charge displacement curve ΔQ , which can be used to determine the direction of the charge transfer, is given by integrating $\Delta\rho_{avg}(z)$ along z-direction as follows:

$$\Delta Q = \int_0^z \Delta\rho_{avg}(z) dz$$
(6)

the negative value of ΔQ represents that the electrons are transferred along the positive direction of the z-axis, and the positive value corresponds to the electron transfer along the negative direction of the z-axis.

Diffusion coefficient. The mean square displacement (MSD) function, which increases linearly with time in gaseous or liquid phase system with free motion of atoms, is used to calculate the diffusion coefficient (D):

$$D = \frac{1}{6N} \lim_{t \rightarrow \infty} \frac{d}{dt} \sum_{i=1}^{N_\alpha} \langle [r_i(t) - r_i(0)]^2 \rangle$$
(7)

where $\langle \cdot \rangle$ represents an average over all the guest molecules, $r_i(t)$ and $r_i(0)$ denote the position vector of the analyte molecule i in space at time t and its initial position, respectively. These calculations are executed by using VASPKIT code.⁴

Experimental details

Colloidal synthesis of undoped and Na-doped CsSn_{0.6}Pb_{0.4}I₃ QDs.¹ 0.75 g of SnI₂ (99%, Wako Pure Chemicals, Japan) and 0.25 g of PbI₂ (99%, Sigma-Aldrich, USA) were mixed into 2.5 mL of tri-n-octylphosphine (TOP, 97%, Sigma-Aldrich, USA). The mixture was vigorously stirred on a hot plate at 90 °C for about 2 h. In a 50 mL three-neck flask, 0.07 g of Cs₂CO₃ (99.9%, Sigma-Aldrich, USA), 0.4 mL of oleic acid (≥ 65.0%, Wako Pure Chemicals, Japan), and 0.4 mL of oleylamine (70%, Sigma-Aldrich, USA) were mixed into 12 mL of octadecene (90%, Sigma-Aldrich, USA). The mixture was heated at 100 °C with vigorous stirring under vacuum for 30 min and then heated to 120 °C under nitrogen until the solution became clear. For Na doping, after the complete dissolution of Cs₂CO₃, the solution was first cooled down to room temperature and 0.06~0.13 g of sodium acetate trihydrate was added. The solution was then again heated to 120 °C under nitrogen for 20 min until the Na salt was completely dissolved. For both undoped and Na-doped synthesis, the temperature

was raised to 165 °C followed by quick injection of the above prepared TOP-SnI₂-PbI₂ solution. About 5 secs after injection, the reaction was quenched by immediate immersion of the flask into an ice bath. After cooling, the crude solution was transferred to centrifuge tubes and to each tube three volumes of methyl acetate (MeOAc, anhydrous 99.5%, Sigma-Aldrich, USA) were added to precipitate the QDs, followed by centrifugation at 4000 rpm for 2 min. The supernatant was discarded and the QD precipitate was dispersed in hexane.

Characterization. X-ray photoelectron spectroscopy (XPS) data were accumulated on a photoelectron spectrometer, JPS-90MX (JEOL, Ltd., Japan).

Table S1. The comparison of ligand density with experimental data.

	¹ H NMR and calculation ⁵	Our model
Total ligand density	1.70	1.24
R-NH ₃ ⁺ ligand density ^a	1.00	0.62
Oleate density	0.62	0.62

^a CsPbBr₃ QDs with ammonium ligand dodecylammonium (DDA). The oleate densities are the same. The R-NH₃⁺ ligand density and the total ligand density is lower than the measurement. The OLA ligand is longer than DDA in the reference paper, which indicates that the lower R-NH₃⁺ ligand density in our work is reasonable. Thus, the feasibility of our model is validated. The unit of the ligand density is in ligand/nm².

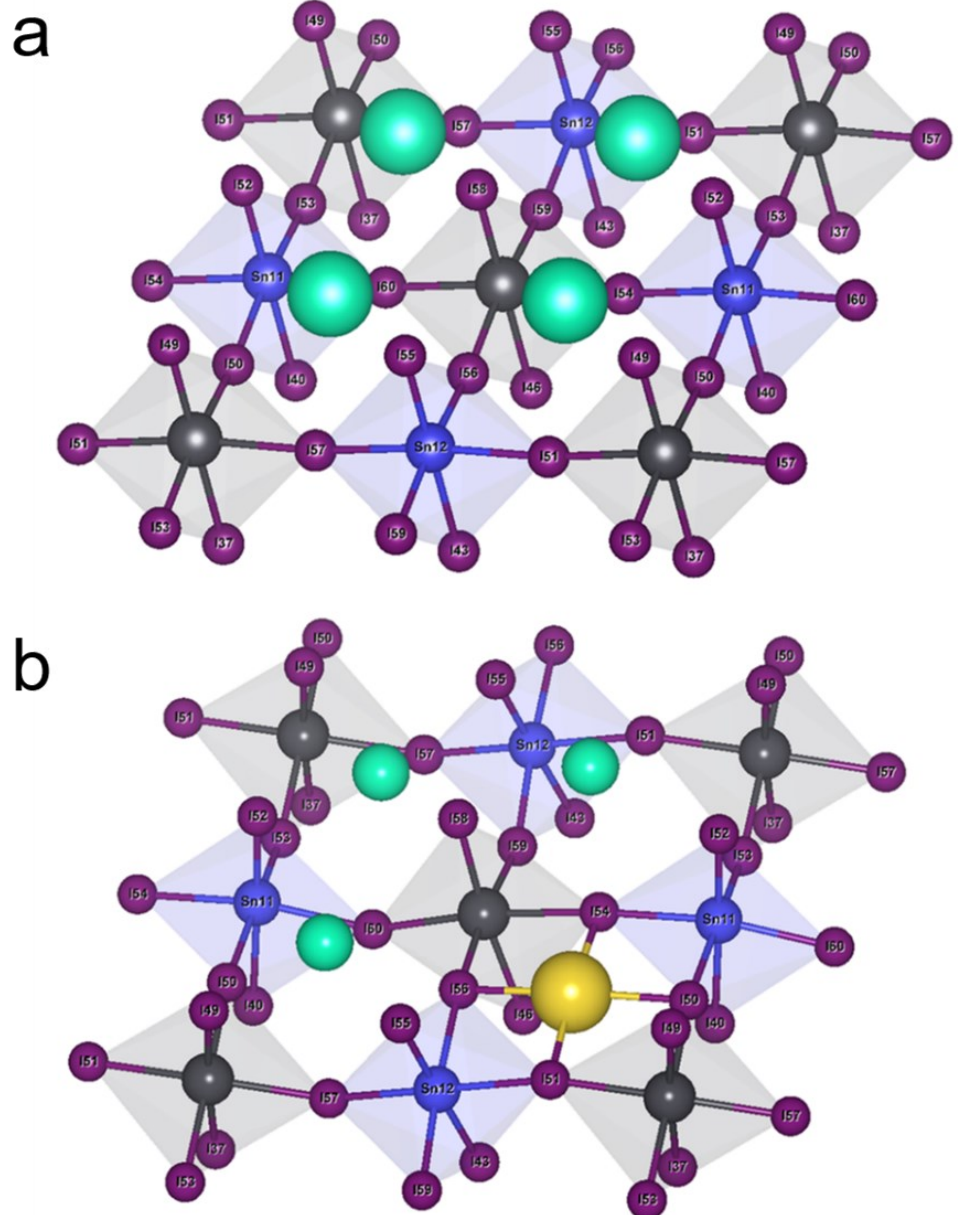


Figure S1. Atomistic view of the CsI-terminated surface of $\text{CsSn}_{0.6}\text{Pb}_{0.4}\text{I}_3$ perovskite (a) without and (b) with the incorporation of Na^+ ions.

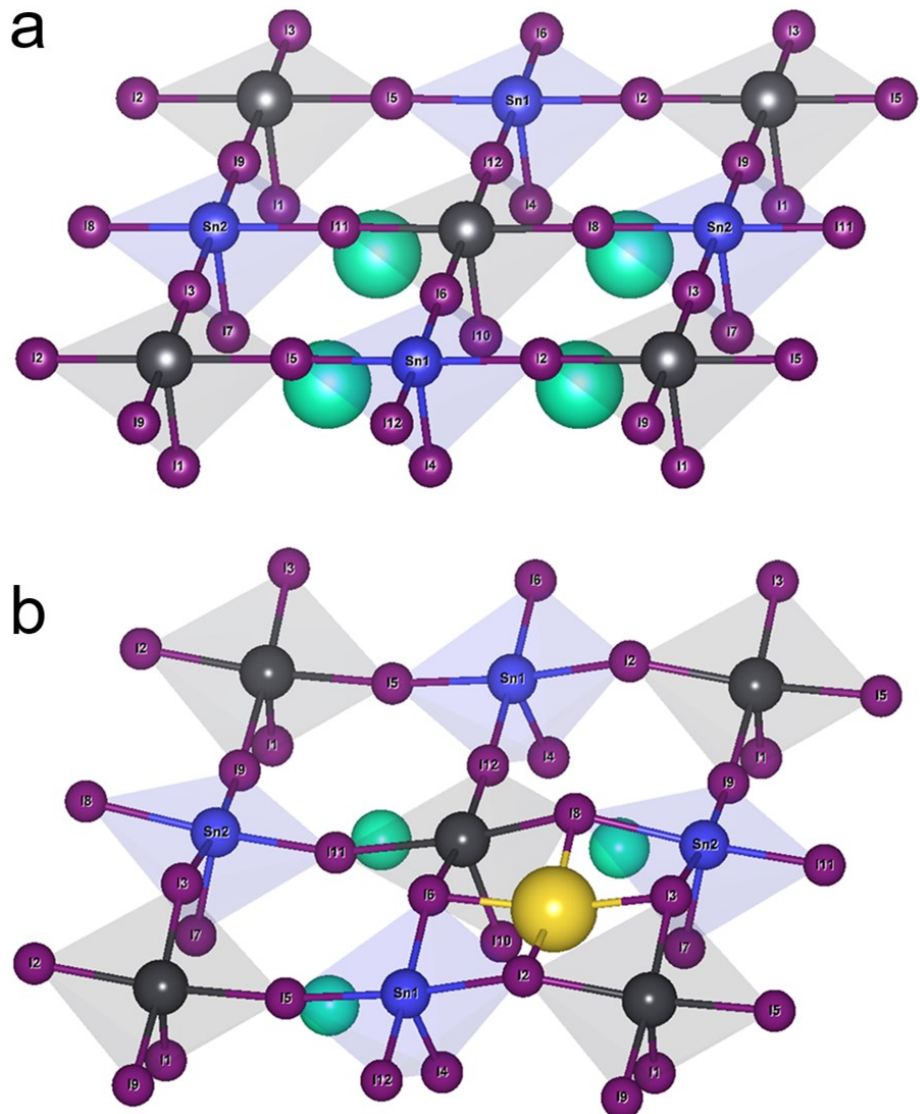


Figure S2. Atomistic view of the MI_2 -terminated surface of $\text{CsSn}_{0.6}\text{Pb}_{0.4}\text{I}_3$ perovskite (a) without and (b) with incorporation of Na^+ ions.

Table S2. Detailed information of bond length and bond order between atoms, and net atomic charge of each atom in Figure S1 (CsI-terminated surface).

Bond Length	Sn11/I50	Sn11/I52	Sn11/I53	Sn11/I54	Sn11/I60	Sn12/I51	
undoped	3.15	3.01	3.15	3.15	3.15	3.14	
Na-doped	3.22	2.94	3.16	3.22	3.16	3.22	
/	Sn12/I55	Sn12/I56	Sn12/I57	Sn12/I59	Cs(Na)/I50	Cs(Na)/I51	
undoped	3.01	3.14	3.14	3.14	Cs17/I50: 4.00	Cs17/I51: 4.01	
Na-doped	3.02	3.22	3.16	3.16	Na/I50: 3.18	Na/I51: 3.11	
Bond Order	Sn11/I50	Sn11/I52	Sn11/I53	Sn11/I54	Sn11/I60	Sn12/I51	
undoped	0.44	0.60	0.44	0.44	0.44	0.44	
Na-doped	0.39	0.66	0.44	0.39	0.44	0.40	
/	Sn12/I55	Sn12/I56	Sn12/I57	Sn12/I59	Cs(Na)/I50	Cs(Na)/I51	
undoped	0.60	0.44	0.44	0.44	Cs17/I50: 0.10	Cs17/I51: 0.10	
Na-doped	0.58	0.40	0.44	0.44	Na/I50: 0.12	Na/I51: 0.14	
Net Atomic Charge	Sn-11	Sn-12	I-50	I-51	I-52	I-53	I-54
undoped	0.71	0.70	-0.52	-0.53	-0.55	-0.53	-0.53
Na-doped	0.70	0.70	-0.56	-0.55	-0.48	-0.51	-0.56
/	I-55	I-56	I-57	I-58	I-59	I-60	/
undoped	-0.55	-0.53	-0.53	-0.59	-0.53	-0.53	/
Na-doped	-0.53	-0.55	-0.53	-0.56	-0.53	-0.51	/

Table S3. Detailed information of bond length and bond order between atoms, and net atomic charge of each atom in Figure S2 (MI_2 -terminated surface).

Bond Length	Sn1/I2	Sn1/I4	Sn1/I5	Sn1/I6	Sn2/I3	Sn2/I7	
undoped	3.14	2.95	3.14	3.14	3.14	2.96	
Na-doped	3.20	2.92	3.16	3.20	3.35	2.93	
/	Sn2/I8	Sn2/I9	Sn2/I1	Cs(Na)/I6	Cs(Na)/I8	/	
undoped	3.14	3.14	3.14	Cs1/I6: 4.08	Cs1/I8: 4.10	/	
Na-doped	3.35	3.10	3.10	Na/I6: 3.20	Na/I8: 3.17	/	
Bond Order	Sn1/I2	Sn1/I4	Sn1/I5	Sn1/I6	Sn2/I3	Sn2/I7	
undoped	0.47	0.61	0.47	0.47	0.46	0.59	
Na-doped	0.43	0.65	0.46	0.43	0.35	0.65	
/	Sn2/I8	Sn2/I9	Sn2/I1	Cs(Na)/I6	Cs(Na)/I8	/	
undoped	0.46	0.46	0.46	Cs1/I6: 0.09	Cs1/I8: 0.08	/	
Na-doped	0.35	0.51	0.51	Na/I6: 0.12	Na/I8: 0.13	/	
Net Atomic Charge	Sn-1	Sn-2	I-2	I-3	I-4	I-5	I-6
undoped	0.71	0.72	-0.50	-0.50	-0.46	-0.50	-0.50
Na-doped	0.69	0.69	-0.51	-0.51	-0.41	-0.51	-0.51
/	I-7	I-8	I-9	I-10	I-11	I-12	/
undoped	-0.48	-0.50	-0.50	-0.49	-0.50	-0.50	/
Na-doped	-0.39	-0.51	-0.51	-0.43	-0.51	-0.51	/

Table S4. The surface atomistic composition of $\text{CsSn}_{0.6}\text{Pb}_{0.4}\text{I}_3$ QDs excludes the ligands, showed by XPS.

Element	Cs	Pb	Sn	I	I/Cs
Atomistic %	21.71	14.64	6.05	57.60	2.65

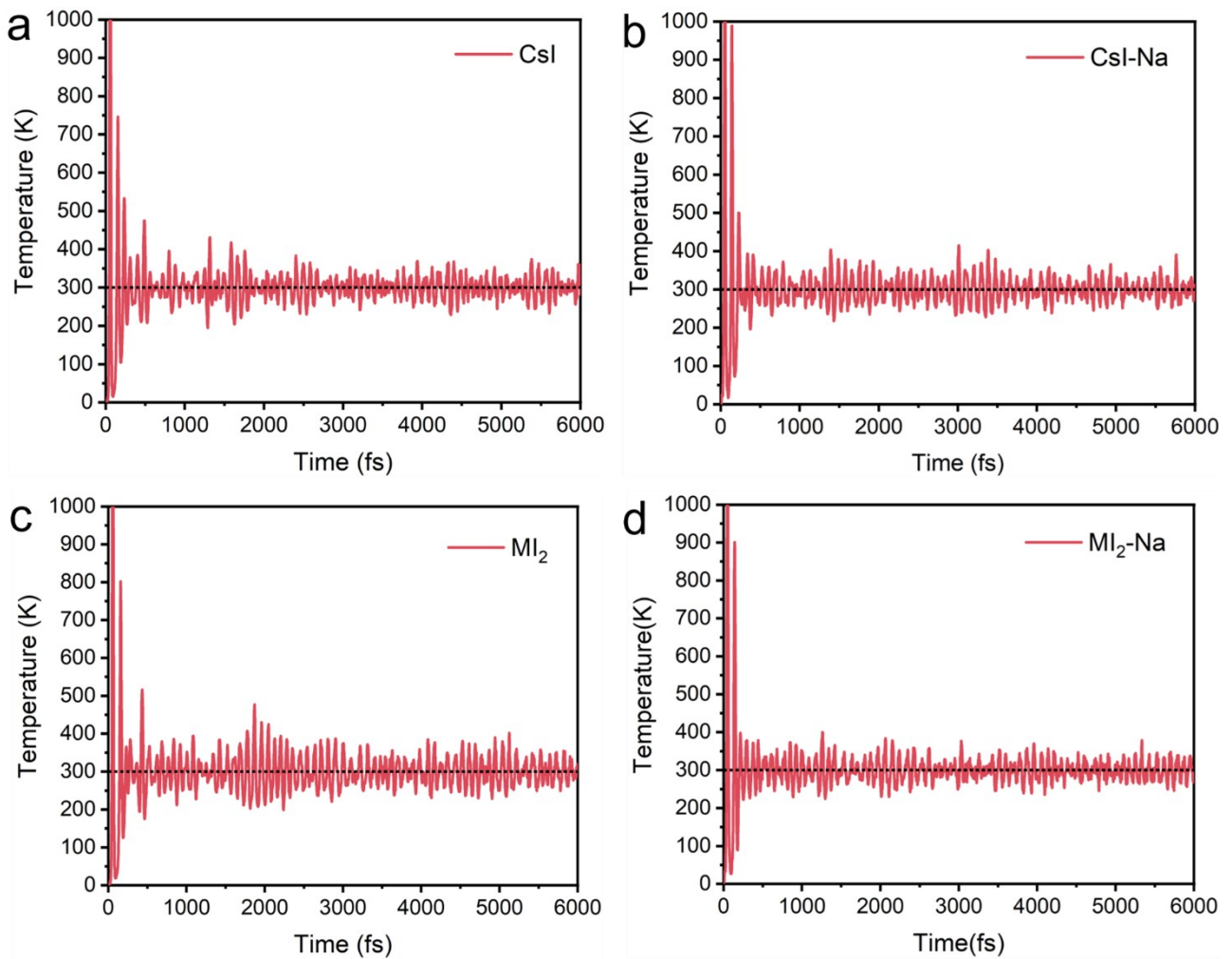


Figure S3. The simulated temperature of CsI-terminated surface model (a) without and (b) with Na doping, and MI₂-terminated surface model (c) without and (d) with Na doping. These figures show that the simulations reach an equilibrium temperature of 300 K after about 200 fs. Therefore, the trajectory of the first 200 fs in each simulation is depleted for the data analysis.

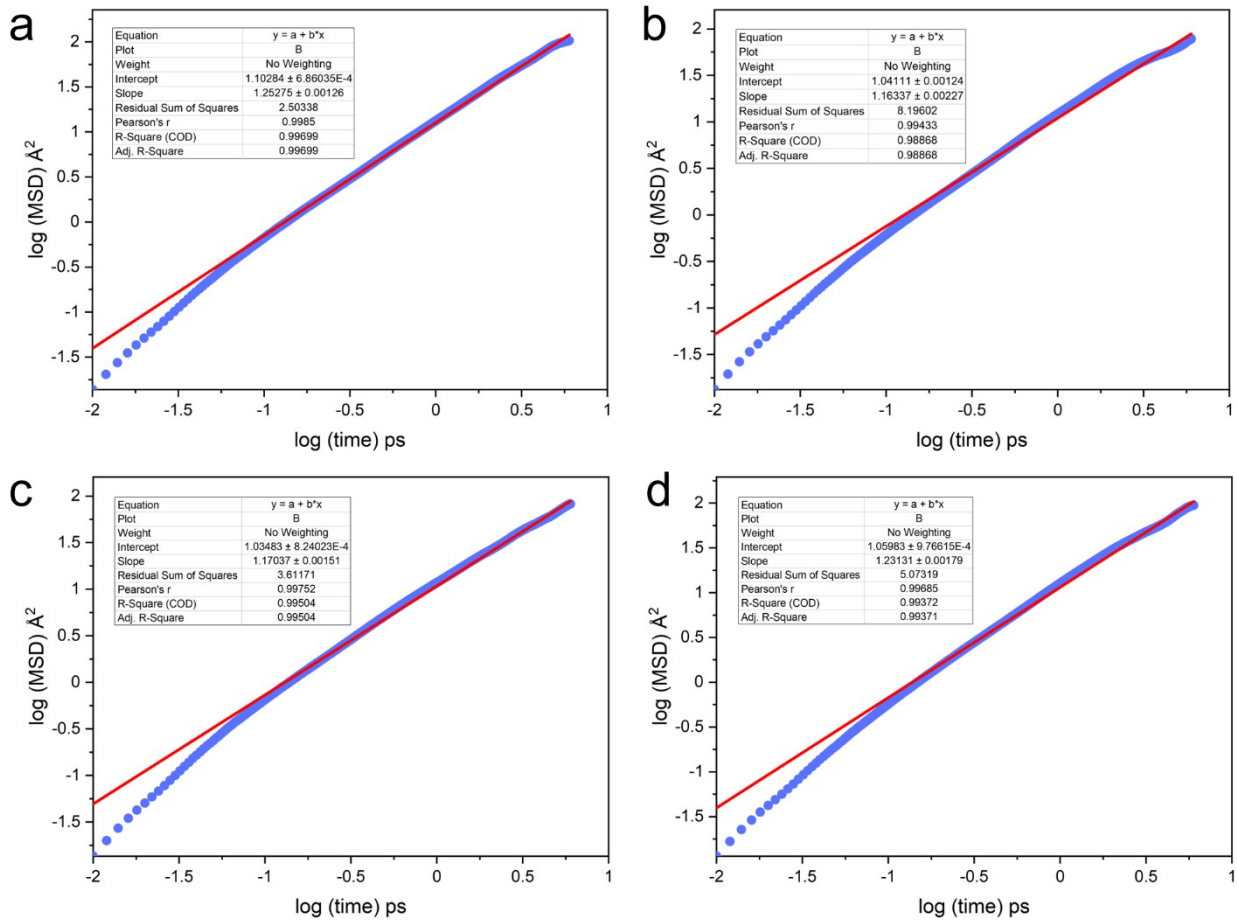


Figure S4. $\log(\text{MSD})$ as a function of $\log(\text{time})$ of for the diffusive ions in (a) CsI, (b) CsI-Na, (c) MI_2 , and (d) $\text{MI}_2\text{-Na}$ surface models. The red line is the linear fit of the data (blue dots).

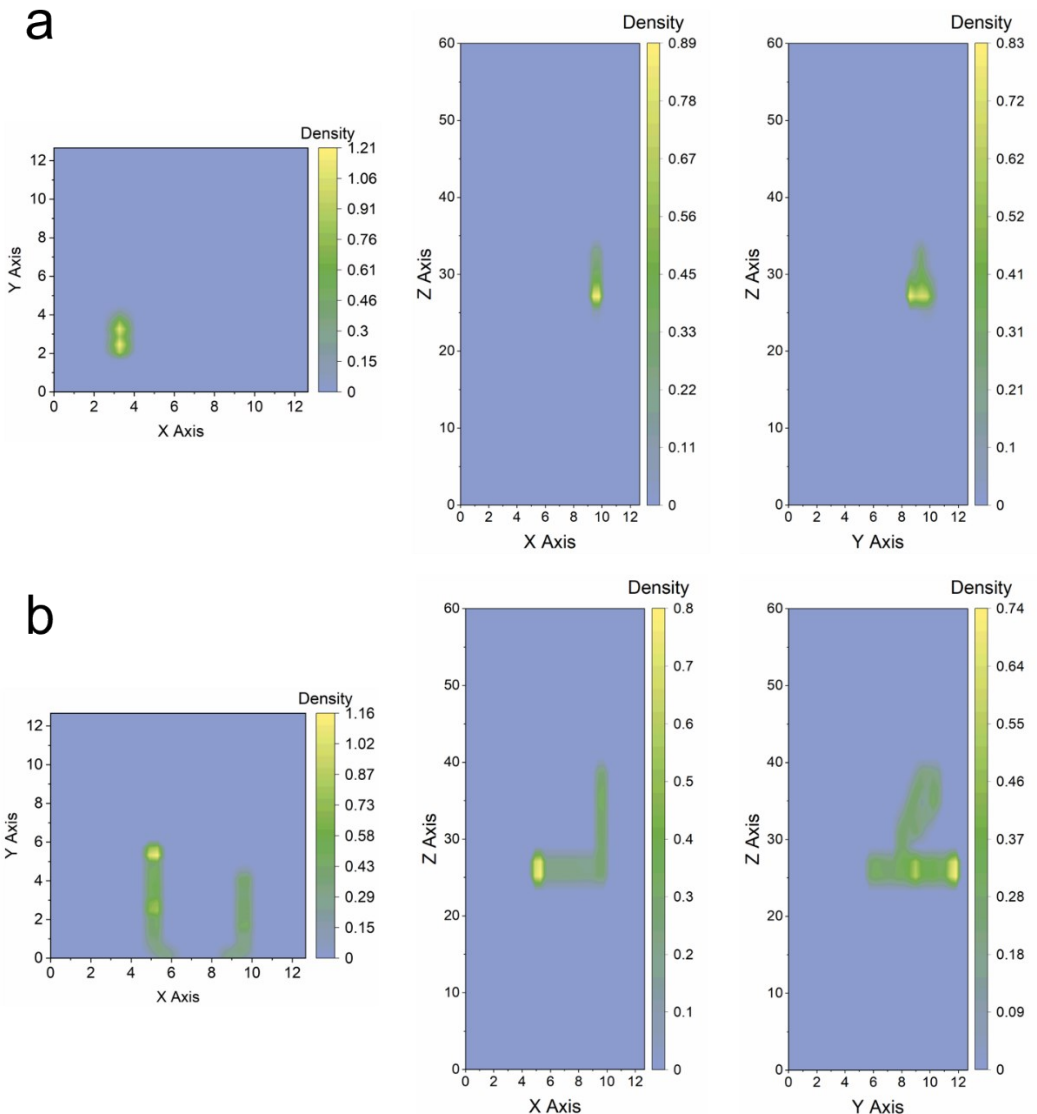


Figure S5. Location distribution density plot of Na⁺ at (a) CsI- and (b) MI₂-terminated surface during 6 ps AIMD simulation (top view, front view, and side view from left to right).

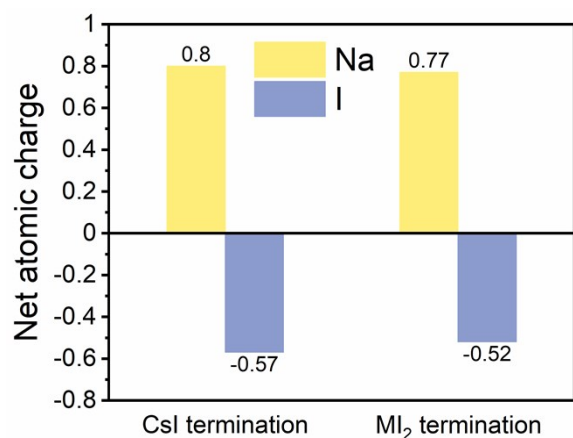


Figure S6. Net atomic charges of the Na⁺ and adjacent I ion for CsI-terminated surface and MI₂-terminated surface, respectively. The value of I is averaged from 4 adjacent atoms of Na.

Effect of introducing other alkaline cations

Encouraged by the positive effect of Na doping, we also investigated the effect of introducing other alkaline cations Li, Na, K, Rb, and Fr and made a comparison with Na. We first determined the possible atomistic locations of alkaline cations in the QDs. Table S5 summarizes the three possible locations of different alkaline cations in the QDs. Similar to Na^+ , the Li^+ , K^+ , and Rb^+ are found to be more stable on surfaces (Li^+ on interstitial site, K^+ and Rb^+ on A site), while the Fr^+ do not show preference of locating on the surface or in the bulk. Generally, the preference of locating on the surface decreases with the increased size of the ions. We then calculated the ligand binding energy with alkaline cations doping on both CsI -termination and MI_2 -termination, and compared with the undoped configuration, see Figure S7. The binding energies show that except for the Na^+ , all other alkaline cations show a negative effect. The binding energies are significantly reduced on CsI -termination and moderately reduced on MI_2 -termination.

Table S5. The energy comparison of alkaline cations doping at various location: in the bulk, on CsI -termination, and on MI_2 -termination, respectively. The energy in the bulk is set to 0 eV for comparison.

Cation type \ Energy (eV)	Bulk	CsI -termination	MI_2 -termination
Li	0	-0.27	-0.29
Na	0	-0.22	-0.26
K	0	-0.22	-0.15
Rb	0	-0.14	-0.07
Fr	0	0	-0.03

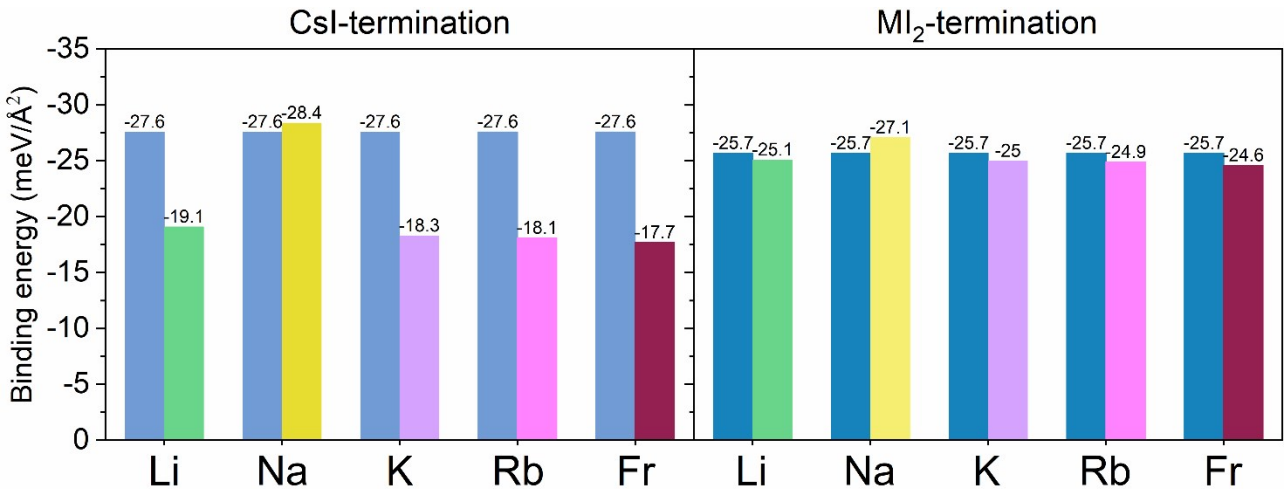


Figure S7. Binding energies of Li, Na, K, Rb, and Fr doping on (a) CsI- and (b) MI₂-termination, respectively. The blue bar denotes the original surface. The green, yellow, violet, pink, and wine-red bars denote the Li, Na, K, Rb, and Fr-incorporated surfaces. The binding energies are calculated by using the most favorable ligands binding mode in each termination. For CsI-termination, the OLA substituting Cs and OA substituting I configuration is used, and for MI₂-termination, the attaching mode of OLA attached to A cation and OA attached to Sn is used.

Optimized crystal structures for $\text{CsSn}_{0.6}\text{Pb}_{0.4}\text{I}_3$ slab model without and with Na-doping at different surface termination, formatted as VASP input POSCAR file as below:

$\text{CsSn}_{0.6}\text{Pb}_{0.4}\text{I}_3$

1.000000000000000	0.000000000000000	0.000000000000000
12.661199569700008	0.000000000000000	0.000000000000000
0.000000000000000	12.661199569700008	0.000000000000000
0.000000000000000	0.000000000000000	44.253799438500033

Cs	Pb	I	Sn
20	8	60	12

Direct

0.2498007487355380	0.2501992512644620	0.2030035917357722
0.7501992512644620	0.2501992512644620	0.2030035917357722
0.2498007487355380	0.7498007487355380	0.2030035917357722
0.7501992512644620	0.7498007487355380	0.2030035917357722
0.2506289183298307	0.2493710816701693	0.3508496279435818
0.7493710816701693	0.2493710816701693	0.3508496279435818
0.2506289183298307	0.7506289183298307	0.3508496279435818
0.7493710816701693	0.7506289183298307	0.3508496279435818
0.2493802405478647	0.2506197594521353	0.4949153990126405
0.7506197594521353	0.2506197594521353	0.4949153990126405
0.2493802405478647	0.7493802405478647	0.4949153990126405
0.7506197594521353	0.7493802405478647	0.4949153990126405
0.2491929940897535	0.2508070059102465	0.6341659292271302
0.7508070059102465	0.2508070059102465	0.6341659292271302
0.2491929940897535	0.7491929940897535	0.6341659292271302
0.7508070059102465	0.7491929940897535	0.6341659292271302
0.2496730019007884	0.2503269980992116	0.7701564654755870
0.7503269980992116	0.2503269980992116	0.7701564654755870
0.2496730019007884	0.7496730019007884	0.7701564654755870
0.7503269980992116	0.7496730019007884	0.7701564654755870
0.000000000000000	0.000000000000000	0.1454304603706760
0.500000000000000	0.500000000000000	0.1454304603706760
0.000000000000000	0.500000000000000	0.2871963191642735
0.000000000000000	0.000000000000000	0.4296835588837453
0.500000000000000	0.500000000000000	0.4296835588837453
0.500000000000000	0.000000000000000	0.5735876035457466
0.000000000000000	0.000000000000000	0.7198992090958924
0.500000000000000	0.500000000000000	0.7198992090958924
0.000000000000000	0.000000000000000	0.2139250052567903
0.2521795912561799	0.000000000000000	0.1449816299824818
0.000000000000000	0.2519689232683930	0.1439517743687091
0.500000000000000	0.000000000000000	0.2133778786200438
0.7478204087438201	0.000000000000000	0.1449816299824818
0.500000000000000	0.2478204087438201	0.1449816299824818
0.000000000000000	0.500000000000000	0.2111230616948063
0.2480310767316070	0.500000000000000	0.1439517743687091

0.0000000000000000	0.7480310767316070	0.1439517743687091
0.5000000000000000	0.5000000000000000	0.2139250052567903
0.7519689232683930	0.5000000000000000	0.1439517743687091
0.5000000000000000	0.7521795912561799	0.1449816299824818
0.0000000000000000	0.0000000000000000	0.3559385870647986
0.2500943808354705	0.0000000000000000	0.2867658936179041
0.0000000000000000	0.2476296178886983	0.2862747400389551
0.5000000000000000	0.0000000000000000	0.3561428380432901
0.7499056191645295	0.0000000000000000	0.2867658936179041
0.5000000000000000	0.2499056191645295	0.2867658936179041
0.0000000000000000	0.5000000000000000	0.3573973475890568
0.2523703821113017	0.5000000000000000	0.2862747400389551
0.0000000000000000	0.7523703821113017	0.2862747400389551
0.5000000000000000	0.5000000000000000	0.3559385870647986
0.7476296178886983	0.5000000000000000	0.2862747400389551
0.5000000000000000	0.7500943808354705	0.2867658936179041
0.0000000000000000	0.0000000000000000	0.5008803137321181
0.2522718583588741	0.0000000000000000	0.4282870458163544
0.0000000000000000	0.2523129345693675	0.4299841086145264
0.5000000000000000	0.0000000000000000	0.4985371968376242
0.7477281416411259	0.0000000000000000	0.4282870458163544
0.5000000000000000	0.2477281416411259	0.4282870458163544
0.0000000000000000	0.5000000000000000	0.4999415923348707
0.2476870654306325	0.5000000000000000	0.4299841086145264
0.0000000000000000	0.7476870654306325	0.4299841086145264
0.5000000000000000	0.5000000000000000	0.5008803137321181
0.7523129345693675	0.5000000000000000	0.4299841086145264
0.5000000000000000	0.7522718583588741	0.4282870458163544
0.0000000000000000	0.0000000000000000	0.6428835948875076
0.2477118234903486	0.0000000000000000	0.5716026791972268
0.0000000000000000	0.2501235571132909	0.5719181448962445
0.5000000000000000	0.0000000000000000	0.6439204513528125
0.7522881765096514	0.0000000000000000	0.5716026791972268
0.5000000000000000	0.2522881765096514	0.5716026791972268
0.0000000000000000	0.5000000000000000	0.6422871099396303
0.2498764428867091	0.5000000000000000	0.5719181448962445
0.0000000000000000	0.7498764428867091	0.5719181448962445
0.5000000000000000	0.5000000000000000	0.6428835948875076
0.7501235571132909	0.5000000000000000	0.5719181448962445
0.5000000000000000	0.7477118234903486	0.5716026791972268
0.0000000000000000	0.0000000000000000	0.7897429106934624
0.2521919140475433	0.0000000000000000	0.7150693696173036
0.0000000000000000	0.2522389379861920	0.7142566231374019
0.5000000000000000	0.0000000000000000	0.7880825916668215
0.7478080859524567	0.0000000000000000	0.7150693696173036
0.5000000000000000	0.2478080859524567	0.7150693696173036
0.0000000000000000	0.5000000000000000	0.7867399094367471
0.2477610620138080	0.5000000000000000	0.7142566231374019

0.0000000000000000	0.7477610620138080	0.7142566231374019
0.5000000000000000	0.5000000000000000	0.7897429106934624
0.7522389379861920	0.5000000000000000	0.7142566231374019
0.5000000000000000	0.7521919140475433	0.7150693696173036
0.5000000000000000	0.0000000000000000	0.1467184102746728
0.0000000000000000	0.5000000000000000	0.1442972374790799
0.0000000000000000	0.0000000000000000	0.2868662392126282
0.5000000000000000	0.0000000000000000	0.2878122861240726
0.5000000000000000	0.5000000000000000	0.2868662392126282
0.5000000000000000	0.0000000000000000	0.4293859665677218
0.0000000000000000	0.5000000000000000	0.4307458648284381
0.0000000000000000	0.0000000000000000	0.5734148705872286
0.0000000000000000	0.5000000000000000	0.5734224972714870
0.5000000000000000	0.5000000000000000	0.5734148705872286
0.5000000000000000	0.0000000000000000	0.7200996414420473
0.0000000000000000	0.5000000000000000	0.7187621294898818

Na-doped CsSn_{0.6}Pb_{0.4}I₃ Csl-termination

1.0000000000000000		
12.6611995697000008	0.0000000000000000	0.0000000000000000
0.0000000000000000	12.6611995697000008	0.0000000000000000
0.0000000000000000	0.0000000000000000	44.2537994385000033

Cs	Na	Pb	I	Sn
19	1	8	60	12

Direct

0.2508959497219792	0.2491040502780208	0.2124478126350979
0.7550964153641004	0.2428224297894559	0.2082828874546720
0.2571775702105441	0.7449035846358996	0.2082828874546720
0.7515433100197626	0.7484566899802374	0.1871801932792110
0.2504738790951819	0.2495261209048181	0.3336141354485065
0.7344791002405060	0.2508462941273564	0.3583667798290122
0.2491537058726436	0.7655208997594940	0.3583667798290122
0.7524290145894241	0.7475709854105759	0.3554458712669444
0.2494636948149775	0.2505363051850225	0.4960845552549955
0.7559457672016592	0.2422120989073022	0.5002649884947985
0.2577879010926978	0.7440542327983408	0.5002649884947985
0.7534016800688761	0.7465983199311239	0.4772633727799729
0.2498732824769974	0.2501267175230026	0.6147559542259202
0.7146675731090468	0.2511375010794481	0.6384452358076942
0.2488624989205519	0.7853324268909532	0.6384452358076942
0.7523344735248614	0.7476655264751386	0.6365347347021029
0.7432206924998255	0.2919056494219134	0.7743657405362541
0.2080943505780866	0.7567793075001745	0.7743657405362541
0.7466769257475576	0.7533230742524424	0.7614029340494852
0.2439561956334799	0.2560438043665201	0.7284465702513927

0.0004147750637671	0.9969885970532744	0.1504278070292528
0.5030114029467256	0.4995852249362329	0.1504278070292528
0.0006069638491937	0.4993930361508063	0.2893723018707277
0.0007918235906814	0.0004298574938915	0.4301078632552446
0.4995701425061085	0.4992081764093186	0.4301078632552446
0.5016396144492958	0.9983603855507042	0.5715244841088278
0.9943641241389827	0.9986826804156763	0.7159778955589573
0.5013173195843237	0.5056358758610173	0.7159778955589573
0.9581078945726347	0.9595404587500198	0.2174080412558723
0.2523541358515828	0.9997829342484863	0.1580662351041937
0.0052072813728401	0.2498377508917216	0.1563773466551979
0.5402493008616887	0.9597506991383113	0.2148335264403514
0.7482409327921360	0.0082759081379038	0.1367388639375164
0.5002170657515137	0.2476458831484152	0.1580662351041937
0.9637131090558668	0.5362868909441332	0.2139819265019582
0.2501622491082784	0.4947927186271670	0.1563773466551979
0.0105937096322322	0.7460678308398414	0.1366576313450736
0.5404595412499802	0.5418921054273653	0.2174080412558723
0.7539321691601586	0.4894062903677678	0.1366576313450736
0.4917240918620962	0.7517590672078640	0.1367388639375164
0.0472041186677359	0.0354974358926654	0.3575320031271900
0.2573778403854590	0.9946385980359906	0.2755970786446511
0.0015904062447092	0.2465911284709321	0.2747117601922611
0.4626738345057930	0.0373261654942070	0.3564967001806849
0.7569672246333141	0.0056877465826233	0.3014586564340007
0.5053614019640023	0.2426221596145410	0.2755970786446511
0.0405579467820445	0.4594420532179555	0.3580459365515836
0.2534088715290679	0.4984095937552908	0.2747117601922611
0.0073930076787505	0.7514980445264854	0.3005626964123067
0.4645025641073346	0.4527958813322641	0.3575320031271900
0.7485019554735146	0.4926069923212495	0.3005626964123067
0.4943122534173767	0.7430327753666859	0.3014586564340007
0.9557785614591552	0.9648987427986455	0.5001799726891676
0.2543065567958038	0.9897140089827730	0.4422238066256270
0.9941550207604877	0.2518926396520342	0.4414928679245236
0.5415552987707883	0.9584447012292117	0.4977569422283139
0.7495769473344680	0.9984536194117979	0.4164429060452761
0.5102859910172270	0.2456934622041942	0.4422238066256270
0.9649255323360677	0.5350744676639323	0.4987044346341989
0.2481073793479709	0.5058449792395123	0.4414928679245236
0.0016024491884608	0.7475441883182867	0.4177107854822708
0.5351012572013545	0.5442214385408448	0.5001799726891676
0.7524558116817133	0.4983975508115392	0.4177107854822708
0.5015463805882021	0.7504230526655320	0.4164429060452761
0.0441753887111958	0.0352269816225572	0.6402018829946172
0.2492582243565238	0.9961808425354377	0.5576562640336959
0.0023976938705417	0.2485992791866636	0.5586520663975989
0.4606044677469612	0.0393955322530388	0.6403925889088100

0.7537328410256521	0.0068600821429428	0.5838310363556047
0.5038191574645623	0.2507417946434813	0.5576562640336959
0.0377623067923238	0.4622376932076762	0.6396663213053770
0.2514007208133364	0.4976023061294583	0.5586520663975989
0.0070057551341378	0.7487973180035183	0.5816002733209089
0.4647730183774428	0.4558246112888042	0.6402018829946172
0.7512026819964817	0.4929942448658622	0.5816002733209089
0.4931399178570572	0.7462671589743479	0.5838310363556047
0.9671717934728790	0.9527688851065719	0.7838245822114942
0.2501809926836387	0.0059465966131427	0.7234973992993403
0.9981380811142699	0.2527008755219953	0.7260333649488615
0.5345126537444926	0.9654873462555074	0.7830377903547969
0.7462722008127827	0.0052263513520856	0.7007205935262988
0.4940534033868573	0.2498190073163684	0.7234973992993403
0.9612542729483380	0.5387457270516620	0.7809651154223545
0.2472991244780047	0.5018619188857301	0.7260333649488615
0.0057174952681578	0.7482594583655526	0.6998710616170740
0.5472311148934281	0.5328282065271210	0.7838245822114942
0.7517405416344474	0.4942825047318422	0.6998710616170740
0.4947736486479144	0.7537277991872173	0.7007205935262988
0.5048705708260925	0.9951294291739075	0.1494298452952236
0.9981100790369339	0.5018899209630661	0.1484654597506960
0.9930541292289448	0.9999720281093474	0.2900268027329318
0.4939807091307387	0.0060192908692613	0.2880094463133815
0.5000279718906526	0.5069458707710552	0.2900268027329318
0.4998186132478111	0.0001813867521889	0.4304583888498428
0.0011720644839173	0.4988279355160827	0.4306892993658025
0.9999582167781256	0.9999873379270880	0.5717932526532721
0.0000891516390027	0.4999108483609973	0.5722052971402363
0.5000126620729120	0.5000417832218744	0.5717932526532721
0.5036638875805437	0.9963361124194563	0.7176936381733796
0.9961641687992042	0.5038358312007958	0.7142481688444065

Na-doped CsSn_{0.6}Pb_{0.4}I₃ MI₂-termination

1.00000000000000		
12.6611995697000008	0.0000000000000000	0.0000000000000000
0.0000000000000000	12.6611995697000008	0.0000000000000000
0.0000000000000000	0.0000000000000000	44.2537994385000033
Na Cs Pb I Sn		
1 19 8 60 12		

Direct

0.2429235727323016	0.2570764272676984	0.1438731297742425
0.7363336612134710	0.2447756412358121	0.2154632617737915
0.2552243587641879	0.7636663387865290	0.2154632617737915
0.7403268386030041	0.7596731613969959	0.2130460450279856

0.2517451610512985	0.2482548389487015	0.3540647216381360
0.7457689865539805	0.2660849420333251	0.3585788897548705
0.2339150579666750	0.7542310134460195	0.3585788897548705
0.7491712700951046	0.7508287299048954	0.3341537573564404
0.2476790557180547	0.2523209442819452	0.4774007166561141
0.7511388020023976	0.2521036259861834	0.5014079869801505
0.2478963740138165	0.7488611979976024	0.5014079869801505
0.7554729463297780	0.7445270536702220	0.4972401890754784
0.2432290934259150	0.2567709065740850	0.6370746857331622
0.7584372307079902	0.2296232739871564	0.6389894580747212
0.2703767260128436	0.7415627692920098	0.6389894580747212
0.7600503764442280	0.7399496235557720	0.6223523031903091
0.2490377764696671	0.2509622235303328	0.7643609269358854
0.7266393083077213	0.2583543288240334	0.7706514049994262
0.2416456711759665	0.7733606916922787	0.7706514049994262
0.7650264261077290	0.7349735738922710	0.7705319308217791
0.9980344824393378	0.0121453223600243	0.1516241692316967
0.4878546776399757	0.5019655175606693	0.1516241692316967
0.0008949175334494	0.4991050824665434	0.2865934658254904
-0.0000212391106800	0.9978825012341677	0.4290745040877300
0.5021174987658323	0.5000212391106800	0.4290745040877300
0.5039178318915479	0.9960821681084521	0.5720583910110260
0.0026793870363093	0.9999093232419631	0.7154762096534200
0.5000906767580298	0.4973206129636907	0.7154762096534200
0.0323024943575148	0.0665745253959920	0.2172671725206926
0.2470272497579215	0.0064340937955875	0.1353762458139348
0.9962913867081921	0.2522373914519083	0.1312931998872683
0.4600024932437602	0.0399975067562398	0.2146574711035432
0.7434356334546529	0.0071997139335322	0.1561862211008992
0.4935659062044125	0.2529727692420765	0.1353762458139348
0.0525741148217512	0.4474258851782488	0.2137976595355512
0.2477626085480916	0.5037086132918079	0.1312931998872683
0.0024782218085561	0.7487078898834936	0.1625307152574539
0.4334254746040081	0.4676975056424852	0.2172671725206926
0.7512921101165064	0.4975217781914439	0.1625307152574539
0.4928002860664678	0.7565643665453471	0.1561862211008992
0.9661990673439591	0.9529636345737731	0.3564757968633713
0.2456707471417680	0.9916175648178657	0.2975694739786732
0.9907690766341122	0.2468824562480556	0.3018685857850680
0.5354292815210270	0.9645707184789730	0.3564821034329016
0.7455405455693833	0.0023669127453004	0.2769941417339413
0.5083824351821343	0.2543292528582320	0.2975694739786732
0.9603256695406440	0.5396743304593560	0.3563767639778931
0.2531175437519444	0.5092309233658878	0.3018685857850680
0.9980948141888520	0.7518754589016321	0.2732732153668866
0.5470363654262340	0.5338009326560409	0.3564757968633713
0.7481245410983679	0.5019051858111480	0.2732732153668866
0.4976330872546995	0.7544594544306167	0.2769941417339413

0.0489630389671616	0.0273165414784323	0.4995563686351886
0.2519754730564029	0.0032507129854248	0.4163009741011742
0.0000000919978609	0.2510620110156381	0.4163612600045977
0.4605099946666854	0.0394900053333146	0.4982386918908734
0.7474660420265333	0.0074966380881695	0.4426193758058982
0.4967492870145752	0.2480245459435951	0.4163009741011742
0.0339569391691420	0.4660430608308579	0.4971712727608271
0.2489380079843670	0.4999999080021321	0.4163612600045977
0.0092228206821467	0.7467388455777573	0.4404017689772183
0.4726834585215677	0.4510369610328384	0.4995563686351886
0.7532611544222427	0.4907771793178534	0.4404017689772183
0.4925033619118305	0.7525339579734667	0.4426193758058982
0.9578857698605029	0.9773510707811275	0.6401882949588622
0.2505704041790802	0.9909625309447345	0.5850955205502747
0.9961774342808698	0.2479929265267015	0.5781822865609075
0.5456543190374665	0.9543456809625335	0.6412470133822487
0.7551969250703083	0.9962501744265116	0.5579824101132318
0.5090374690552655	0.2494296148209250	0.5850955205502747
0.9798231627714628	0.5201768372285372	0.6393175488972288
0.2520070734732985	0.5038225657191302	0.5781822865609075
0.0028395711440548	0.7482057137891054	0.5616296343105137
0.5226489292188725	0.5421142301394971	0.6401882949588622
0.7517942862108946	0.4971604288559452	0.5616296343105137
0.5037498255734884	0.7448030749296917	0.5579824101132318
0.0421482403301938	0.0095984819610463	0.7850112967341383
0.2543320348034462	0.9950597621752456	0.7011556423664679
0.9999062389392137	0.2506986023883100	0.7057153027465984
0.4659500603912936	0.0340499396087136	0.7826877523992409
0.7498505355244294	0.9998967945098199	0.7262233559814805
0.5049402378247544	0.2456679651965538	0.7011556423664679
0.0162973795390707	0.4837026204609292	0.7833356862645080
0.2493013976116899	0.5000937610607863	0.7057153027465984
0.0040684936704844	0.7464438676037858	0.7163620905459410
0.4904015180389537	0.4578517596698062	0.7850112967341383
0.7535561323962142	0.4959315063295156	0.7163620905459410
0.5001032054901801	0.7501494644755706	0.7262233559814805
0.4947513354603512	0.0052486645396488	0.1501263330102410
0.9935925254810903	0.5064074745189097	0.1521138600915301
0.0024522038764300	0.0023408382869270	0.2881777538385756
0.5018739541842987	0.9981260458157013	0.2890550371202625
0.4976591617130731	0.4975477961235700	0.2881777538385756
0.5015300227750193	0.9984699772249807	0.4308426776974981
0.0000233349208115	0.4999766650791885	0.4282899186840055
0.0056669890691958	0.9965040673005247	0.5711072131549434
0.0055101961510356	0.4944898038489644	0.5710272709085180
0.5034959326994753	0.4943330109308042	0.5711072131549434
0.4999803804951476	0.0000196195048523	0.7157938317341459
0.0021055293232346	0.4978944706767653	0.7154970835629377

Reference

1. F. Liu, J. Jiang, Y. Zhang, C. Ding, T. Toyoda, S. Hayase, R. Wang, S. Tao and Q. Shen, *Angew. Chem. Int. Edit.*, 2020, **59**, 8421-8424.
2. M. I. Saidaminov, J. Kim, A. Jain, R. Quintero-Bermudez, H. Tan, G. Long, F. Tan, A. Johnston, Y. Zhao, O. Voznyy and E. H. Sargent, *Nat. Energy*, 2018, **3**, 648-654.
3. N. Li, S. Tao, Y. Chen, X. Niu, C. K. Onwudinanti, C. Hu, Z. Qiu, Z. Xu, G. Zheng, L. Wang, Y. Zhang, L. Li, H. Liu, Y. Lun, J. Hong, X. Wang, Y. Liu, H. Xie, Y. Gao, Y. Bai, S. Yang, G. Brocks, Q. Chen and H. Zhou, *Nat. Energy*, 2019, **4**, 408-415.
4. V. Wang, N. Xu, J. C. Liu, G. Tang and W.-T. Geng, *arXiv preprint arXiv:1908.08269*, 2019.
5. Y. Chen, S. R. Smock, A. H. Flintgruber, F. A. Perras, R. L. Brutcher and A. J. Rossini, *J. Am. Chem. Soc.*, 2020, **142**, 6117-6127.